Mutations in the M4 Domain of *Torpedo californica* Acetylcholine Receptor Dramatically Alter Ion Channel Function

Yung-Hui Lee,* Lian Li,* Jose Lasalde,* Lejier Rojas,‡ Mark McNamee,* Sonia I. Ortiz-Miranda,§ and Pamela Pappone§

*Section of Molecular and Cellular Biology and §Section of Neurobiology, Physiology and Behavior, University of California, Davis, California 95616 USA; and ‡Cell Biology Center, Central University of Venezuela, Caracas, Venezuela

ABSTRACT Site-directed mutagenesis was used to mutate αCys418 and βCys447 in the M4 domain of *Torpedo californica* acetylcholine receptor expressed in *Xenopus laevis* oocytes. The M4 region is a transmembrane domain thought to be located at the lipid-protein interface. By whole-cell voltage clamp analysis, mutation of both α subunits to αTrp418 increased maximal channel activity approximately threefold, increased the desensitization rate compared with wild-type receptor, and shifted the EC_{50} for acetylcholine from 32 μM to 13 μM. Patch measurements of single-channel currents revealed that the αTrp418 increased channel open times ~28-fold at 13°C with no effect on channel conductance. All of our measured functional changes in the αTrp418 mutant are consistent with a simple kinetic model of the acetylcholine receptor in which only the channel closing rate is altered by the mutation. Our results show that changes in protein structure at the putative lipid-protein interface can dramatically affect receptor function.

INTRODUCTION

The nicotinic acetylcholine receptor (AChR) is a ligand-gated and cation-selective ion channel protein located in the postsynaptic membranes of many nerve, muscle, and fish electric organ cells. AChR from the marine electric ray *Torpedo californica* can be easily obtained in large quantities, and its structural and biochemical features have been extensively characterized. The *Torpedo* AChR is a multi-subunit integral membrane glycoprotein with four homologous polypeptide subunits, designated α, β, γ, and δ, with a relative stoichiometric ratio of $\alpha_2\beta\gamma\delta$ (for recent reviews see Stroud et al., 1990; Galzi et al., 1991; Lingle et al., 1992; Pradier and McNamee, 1992; Unwin, 1993a). A generally accepted model for the topology of all subunits assumes that the transmembrane domains of each subunit are composed of four hydrophobic domains (M1, M2, M3, M4) (Claudio et al., 1983; Devillers-Thiery et al., 1983; Noda et al., 1983), and that both the N- and C-terminals are located on the extracellular side (DiPaola et al., 1989; see Fig. 1). The M2 transmembrane segment of each subunit is believed to form the lining of the aqueous channel pore (Hucho et al., 1986; Imoto et al., 1988; Leonard et al., 1988; Charnet et al., 1990; Revah et al., 1990, 1991; Villarroel et al., 1991; Bertrand et al., 1992; Pedersen et al., 1992; Villarroel and Sakmann, 1992), but the functions of the other domains are not clear.

To understand the interrelationship between structure and function is an important challenge in characterizing the mechanism of action of the AChR. Selective chemical modifications of cysteine residues in the AChR have been used over the past 20 years as a powerful approach to probe structure-function relationships (Huganir and Racker, 1982; Kao et al., 1984; Clarke and Martinez-Carrion, 1986; Kao and Karlin, 1986; Yee et al., 1986; Mosckovitz and Gershoni, 1988; Marquez et al., 1989). Early attention focused on the pair of cysteines at the ACh binding site (Kao et al., 1984; Kao and Karlin, 1986). In addition, chemical modification of free thiol groups by either *N*-(1-pyrenyl)maleimide (PM) or *N*-phenylmaleimide (NPM) of *Torpedo* AChR under nonreducing conditions led to inhibition of ion channel activity without a detectable effect on ligand binding (Clarke and Martinez-Carrion, 1986; Yee et al., 1986).

Efforts to resolve which cysteines are located in functionally sensitive domains have continued. The γCys416 and γCys420 residues in the amphipathic MA helix located in the cytoplasmic domain between the M3 and M4 segment of the γ subunit and the γCys451 in the M4 transmembrane segment have been identified as the principal sites labeled by NPM. These sites have been studied by site-directed mutagenesis and expression in *Xenopus laevis* oocytes (Pradier et al., 1989; Li et al., 1990). Mutations of the γCys416 and/or γCys420 to Phe or Ser did not show significant functional effects (Pradier et al. 1989), whereas mutations of the γCys451 to Phe or Ser showed substantial inhibition of the channel activity (Li et al., 1990) as measured electrophysiologically by whole-cell current responses to ACh. A cysteine in the M1 transmembrane segment of the α subunit (αCys222) can be selectively labeled by PM (Marquez et al. 1989), and mutation of this Cys to Ser (Mishina et al., 1985) in *Torpedo* AChR or mutation of an equivalent cysteine in the α subunit of murine AChR to Ser (Lo et al., 1991) resulted in no functional changes of the receptors.

Received for publication 28 June 1993 and in final form 10 December 1993.

Address reprint requests to Dr. Mark McNamee, Division of Biological Sciences, Section of Molecular and Cellular Biology, University of California, Davis, CA 95616.

Dr. Li's present address is Laboratory of Molecular and Cellular Neuroscience, Rockefeller University, New York, NY 10021.

Abbreviations used: ACh, acetylcholine; AChR, acetylcholine receptor; NPM, *N*-phenylmaleimide; PM, *N*-(1-pyrenyl)maleimide; PCR, polymerase chain reaction.

0006-3495/94/03/646/08 $2.00

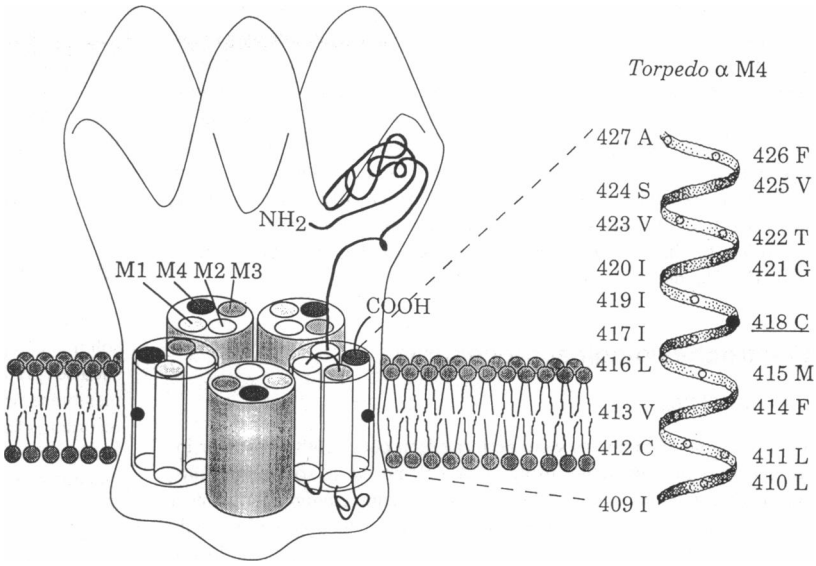

FIGURE 1 Position of the αCys418 in the globular AChR. The two α subunits are shown white, and the β, γ, and δ subunits are dark. Each subunit has four putative transmembrane domains (M1-M4) based on hydropathy plots. The M4 domain is believed to be located at lipid-protein interface and enlarged as an α-helix here. The position of the αCys418 is shown as (●) and is about in the center of M4.

The inhibitory effects of alterations of cysteine residues in the M4 region are somewhat surprising, since the M4 region is believed to be located at the lipid-protein interface based on independent chemical labeling studies (Giraudat et al., 1985; Blanton and Cohen, 1992; see Fig. 1). In the work presented here, we examine the functional roles of other cysteines at the presumed lipid-protein interface in *Torpedo* AChR. The cysteine equivalent to the αCys418 in *Torpedo* is highly conserved among the α subunits from different species and in the *Torpedo* β subunit. The chemical status of the αCys418 and αCys412 in *Torpedo* AChR remain uncertain, since they are insensitive to alkylating agents and could be disulfide bond-linked, fatty acylated, or unusually unreactive (Mosckovitz and Gershoni, 1988). Fig. 1 shows the relative position of the αCys418 in a schematic representation of AChR structure. In this paper, we focus on different amino acid substitutions of the Cys418 in the α subunit of *Torpedo* AChR and a similar cysteine in the β subunit (βCys447) to investigate structure-function relationships involving the M4 domain. In preliminary experiments we observed an increase in the normalized whole-cell current responses for the αTrp418 mutant at very low ACh concentrations (Li et al., 1992). Our present whole-cell voltage clamp and single-channel current measurements reveal that mutations in the M4 region lead to dramatic changes in several aspects of AChR function, including maximum normalized channel activity, desensitization rates, EC_{50} of the ACh dose-response curve, and mean channel open times.

MATERIALS AND METHODS

Materials

Enzymes for recombinant DNA manipulation were purchased from New England Biolabs (Beverly, MA). *Taq* DNA polymerase and DNA amplification kits were from Perkin-Elmer Cetus (Norwalk, CT). Oligonucleotides for polymerase chain reaction (PCR) and DNA sequencing were ordered from American Synthesis (Pleasanton, CA). All other reagents were obtained from standard suppliers.

Mutations on the α and β subunit of *Torpedo* AChR

The coding region of the α subunit of *Torpedo* AChR was subcloned from pα (Pradier et al., 1989) into the *Hin*dIII and *Eco*RI sites of the pGEM3Z(−) vector from Promega (Madison, WI). Directed mutagenesis of the αCys418 was carried out by mismatch amplification using two sequential PCRs (Horton and Pease, 1991). Mutagenic primers were synthesized containing the desired DNA sequence extending about 11 bases on each side of the mismatched region. Flanking primers (~20 mers) were designed to recognize sequences outside the *Bgl*II restriction site in the coding region of the α subunit and the *Eco*RI site on the vector portion of the plasmid. Amplification reactions were performed in a DNA thermal cycler (Perkin-Elmer Cetus) for 30 cycles with denaturation for 1 min at 94°C, annealing for 3 min at 48°C, and polymerization for 3 min at 72°C. The reaction mixture of the first reaction contained 100 μl of 50 mM KCl, 10 mM Tris-HCl (pH 8.3), 1.5 mM $MgCl_2$, 0.01% gelatin, 200 μM each of dNTP, 100 ng DNA plasmid, 1 μg each of primer, and 2.5 units of *Taq* polymerase. The conditions for the second PCR were identical to those for the first one, except that the first PCR products were used instead of the DNA plasmid. The amplified DNA was purified using GeneClean (Bio 101, La Jolla, CA) and then digested with *Bgl*II and *Eco*RI. The final fragment (~900 bp) was purified by GeneClean again and ligated back to the expression plasmid. The resulting mutants were sequenced using the Sequenase 2.0 (United States Biochemical Corp., Cleveland, OH) for double-stranded DNA sequencing to ensure that the desired mutation was present and no undesired base changes had occurred. Mutation for βCys447 was carried out by the same strategy but *Bst*XI and *Sac*II were used as restriction sites.

In vitro RNA transcript synthesis and expression in *X. laevis* oocytes

The linearized cDNA templates of α, β, γ, and δ subunits of *Torpedo* nAChR (pα, pXβ, pXγ, and SP64Tδ) (Pradier et al., 1989) were used for in vitro transcription by SP6 polymerase in the presence of ribonucleotide triphosphates and the cap analogue (m7G(5′)ppp(5′)G, 5′ 7-methyl guanosine residue). Purification of RNA transcripts was performed using Select-D(RF) columns (5 Prime-3 Prime Inc., West Chester, PA) according to the manufacturer's directions.

Ovarian lobes were obtained from anesthetized female *X. laevis* through a ventral incision about 1 cm in length, and the wounds were closed with two or three stitches of sterile catgut. Follicle cell layers were removed by incubation of the oocytes in Ca^{2+}-free OR2 buffer (Wallace et al., 1973) containing 82.5 mM NaCl, 2.5 mM KCl, 1 mM $MgCl_2$, 1 mM Na_2HPO_4,

and 5 mM HEPES, pH 7.6, plus 2 mg/ml collagenase (type 1A, Sigma Chemical Co., St. Louis, MO) for 20 min at room temperature under slow agitation (80–100 rpm) followed by manual defolliculation. Oocytes of stage V or VI were chosen for injection. Fifty nanograms (at a concentration 1 ng/nl) of the α, β, γ, and δ subunit transcripts of *Torpedo* AChR with the ratio of 2:1:1:1 were injected into the cytoplasm of *Xenopus* oocytes. After injection, the oocytes were incubated at 18–19°C in a medium (Heasman et al., 1991) containing 50% Leibovitz's L-15 media (GIBCO, Gaithersburg, MD), 0.4 mg/ml bovine serum albumin; antibiotic-antimycotic was added according to the manufacturer's directions (catalog no. 600–5245AE, GIBCO). The medium was changed daily.

Electrophysiological procedures

Voltage clamp

Voltage clamp experiments were performed on oocytes 48–96 h after injection at room temperature using an Axoclamp 2A (Axon Instruments, Burlingame, CA) in the two-electrode voltage clamp configuration. Under voltage clamp, membrane currents were continuously recorded digitally using the SCAN program (Dagan Corp., Minneapolis, MN) on an 80386-based microcomputer through a TL-1 interface (Axon Instruments). Microelectrodes were prepared using an electrode puller (model P-87, Sutter Instruments, Novato, CA) from 1.5 mm OD/0.84 mm ID glass capillaries (World Precision Instrument, Sarasota, FL, catalog no. 1B150F-4) and filled with 3 M KCl. Voltage electrodes were 10–20 MΩ and current electrodes were about 1 MΩ in resistance. Voltage clamp recordings were made at a holding potential of −80 mV to correspond to the single-channel measurements (see below) with series resistance compensation. The original external buffer in our preliminary reports (Li et al., 1990; Li et al., 1992) was MOR2 buffer (82 mM NaCl, 2.5 mM KCl, 1 mM Na_2HPO_4, 5 mM $MgCl_2$, 0.2 mM $CaCl_2$, and 5 mM HEPES, pH 7.4). To decrease the ACh-induced whole-cell current, the present experiments used an external solution modified from MOR2 buffer by adding EGTA to chelate the free Ca^{2+} and by substituting half of the NaCl concentration with Tris-HCl. The new buffer contained 66 mM Tris-HCl, 41 mM NaCl, 2.5 mM KCl, 1 mM Na_2HPO_4, 5 mM $MgCl_2$, 0.2 mM $CaCl_2$, 5 mM HEPES, and 0.5 mM EGTA, pH 7.4. Solutions containing ACh were freshly prepared immediately before measurement from a 1 M ACh stock solution, which was stored at −20°C. Volume of the oocyte chamber was 1.5 ml. Perfusion rates were 15 ml/min.

The normalized channel activity is defined as the peak of ACh-induced current (nA) per femtomole of surface α-bungarotoxin binding sites (see below). Dose-response measurements for wild-type and each mutant AChR were repeated on at least three oocytes. Data points of dose-response curves were calculated from the peak currents at each concentration. Data points up to 300 μM ACh were fitted with a curve of the form $Y = 100/(1 + (K_d/A)^n)$ using nonlinear regression. Hill coefficients and EC_{50}s (ACh concentrations that give 50% response of maximum normalized activity) were determined from the fitted curves (Table 1). The calculated EC_{50}s and Hill coefficients do not include ACh concentrations higher than 300 μM. By considering that the EC_{50} may be influenced by desensitization of AChR, peak currents were also corrected due to attenuation by desensitization. Fifty percent of the peak responses were taken as zero time (Cachelin and Colquhoun, 1989), and the current traces were fitted with one exponential decay. Corrections for the attenuation were performed by extrapolation of the fitted equation back to zero time to obtain the corrected values of peak current. EC_{50}s from these corrected values were not significantly different from the uncorrected values which are listed in Table 1.

Single-channel recording

Oocytes expressing the *Torpedo* AChR were transferred to a hypertonic solution composed of 150 mM NaCl, 2 mM KCl, 5 mM HEPES, and 3% sucrose (pH 7.6) for 15–30 min to induce osmotic shrinkage. The vitelline membrane was removed manually, and the oocytes were transferred to the recording chamber and washed with 5–10 volumes of a bath solution consisting of 100 mM KCl, 1 mM $MgCl_2$, 10 mM HEPES (pH 7.2). Patch pipettes were made of thick-walled (0.64 mm) borosilicate glass (Sutter Instruments) and had resistances from 7 to 11 MΩ. The pipette (external) solution was composed of 100 mM KCl, 10 mM HEPES, 10 mM EGTA (pH 7.2), and 1–4 μM ACh. Single-channel currents were recorded using the on-cell patch configuration (Hamill et al., 1981) using a L/M-EPC 7 patch-clamp amplifier interfaced to a Cheshire Data Interface and DEC LSI 11/73 computer system (INDEC Systems, Sunnyvale, CA) or a Dagan 3900 amplifier interfaced with a TL-1 DMA (Axon Instruments) to a Everex 386 computer. After a gigaohm seal formation (>10 GΩ), the chamber was cooled to the desired temperature and the data recorded on VHS tapes for later analysis using a modified digital audio processor (VR-10B and VR-10C, Instrutech Corp., Mineola, NY).

Data analysis was performed using pCLAMP software (Axon Instruments) to generate data files. The data reduction step was performed using the IPROC V.3 software programs also distributed by Axon Instruments. All the data generated in this way were filtered at 4 kHz and sampled at 100 μs. Single-channel conductance was calculated from the slope of the current-voltage curves. Open times were calculated from steady-state recordings at −80 mV using a half-amplitude criterion. The measurable short-duration closures in channel openings that are seen in most AChR activity were not evident in our recording, even at higher temporal resolution, indicating that under these conditions there is only one opening per burst.

Radioligand binding assay

Binding assays using [^{125}I]α-bungarotoxin (Amersham Life Sciences, Arlington Heights IL, ~74 TBq/mmol) were performed according to the conditions described by Li et al. (1990). Briefly, the surface binding reactions were performed on the same intact oocytes immediately after the voltage clamp measurement by moving each oocyte into a 80-μl reaction solution containing 1 nM [^{125}I]α-bungarotoxin and 0.5 mg/ml bovine serum albumin. The samples were incubated for 2 h at 25°C and the reaction was

TABLE 1 Functional consequences of αCys418 and βCys447 mutations

AChR mutation	Peak activity	EC_{50}	Hill coefficient*	% peak activity relative to wild type
	(nA/fmol)	μM		
Wild type	225 ± 37 (n = 4)	32 ± 10	1.9 ± 0.4 (n = 4)	100
αTrp418	638 ± 138 (n = 6)	13 ± 3	1.5 ± 0.3 (n = 4)	283
αPhe418	542 ± 157 (n = 4)	18 ± 6	2.6 ± 0.3 (n = 3)	241
αAla418	228 ± 70 (n = 3)	48 ± 7	1.3 ± 0.1 (n = 2)	101
αGly418	121 ± 24 (n = 2)	10 ± 1	2.3 ± 0.2 (n = 2)	54
βTrp447	292 ± 19 (n = 2)	24 ± 9	2.2 ± 0.5 (n = 2)	130

Data are given as means ± S.E. Numbers in parentheses indicate the number of oocytes tested. Normalized peak channel activity for each oocyte was obtained from peak of ACh-induced current (nA) at 300 μM ACh divided by the surface α-bungarotoxin binding data on the same oocyte. Data points from all ACh concentrations were fitted with the Hill equation $Y = 100/(1 + (K_d/A)^n)$. Hill coefficients and EC_{50}s were determined from these fits.

* Hill coefficients from mutants are not significantly different from wild-type receptor by t-test examination.

terminated by washing the oocytes four times with MOR2 buffer. Nonspecific binding was determined by incubating radioactive toxin with uninjected oocytes and was usually less than 5% of the specific binding data. Radioactivity was measured by liquid scintillation counting (Packard Tri-Carb 1500). A calibration curve was obtained by counting 0–20 μl of 1 nM [^{125}I]α-bungarotoxin solution (equivalent to 0–20 fmol).

RESULTS

Mutations of a single cysteine residue on the α subunit alter the size of responses to ACh

Preliminary data in our laboratory showed that the mutation from the αCys418 to Trp dramatically increased the apparent channel activity based on limited voltage clamp experiments at 0.2 and 1 μM ACh (Li et al., 1992). In the experiments presented here, we changed this αCys418 to several different amino acids and carried out a far more extensive electrophysiological analysis to investigate the functional role of this Cys in the M4 domain of AChR. Mutations at the αCys418 position of *T. californica* AChR to Trp, Phe, Ala, or Gly were carried out using directed mutagenesis as described in Materials and Methods. A homologous cysteine in the β subunit was also mutated to Trp by the same strategy. Synthesized oligodeoxynucleotides containing mutated codons of desired mutants were used and two-step PCRs were performed to generate DNA fragments containing the mutations. DNA sequencing was carried out to confirm the entire sequence.

The maximum ACh-induced currents were observed at 300 μM ACh. The maximum channel activities normalized to the number of α-bungarotoxin binding sites for each mutant receptor are listed in Table 1. The results demonstrate that the αTrp418 mutation increases the maximum channel activity to 283% of wild-type AChR, the αPhe418 mutation increases it to 241%, the βTrp447 mutation increases it to 130%, the αGly418 mutation decreases it by ~50%, and the αAla418 mutation gives the similar maximal activity as wild type. Thus mutant receptors with bulky aromatic side chains (Trp and Phe) at the α418 position show larger maximum channel activities and a mutant with a smaller side chain (Gly) decreases channel activity; replacement of αCys418 with Ala, which has a similar size, had little effect on maximum normalized response to ACh.

Because of the dramatic functional increase of this αTrp418 mutant, the whole-cell current saturated our voltage clamp amplifier when responses were obtained at high ACh concentrations in standard buffer solution (MOR2 buffer; see Materials and Methods). To prevent this, the extracellular solution was altered to decrease the current by substituting half of the NaCl concentration with Tris-HCl as described in Materials and Methods. In addition, EGTA was added to chelate the free Ca^{2+} in the extracellular buffer to prevent activation of the Ca^{2+} activated Cl^- channel, which is endogenous in *X. laevis* oocytes (Barish, 1983; Mishina et al., 1985; White et al., 1987). An alternative solution of decreasing the amount of mRNA injected was less desirable, since a consistently high level of AChR expression is required to accurately measure surface bungarotoxin binding. The α-bungarotoxin binding assay is essential for obtaining normalized measurements of channel activity, expressed in nA current per fmole toxin binding sites in each individual oocyte (Li et al., 1990), that can be compared among oocytes and between mutants. By injecting 50 ng of RNA mixture for AChR, we found the typical expression level to be 3.4 ± 1.8 (n = 7) fmol per oocyte. None of our mutants showed alterations in the expression level in the toxin-binding assay. Because the αTrp418 showed very high channel activity, 40 ng of RNA mixture was routinely used for oocyte injection to obtain sufficiently high expression of AChR without saturating our voltage clamp amplifier.

Examples of dose-response curves for wild type and each of the mutant AChRs are shown in Fig. 2. The αTrp418, αPhe418, and βTrp447 AChR mutations increased the normalized response to ACh compared with the wild type at all concentrations from 1 μM to 1 mM ACh. In contrast, the αAla418 mutation slightly decreased the responses at low ACh concentrations, with almost the same maximum response as wild type, and the αGly418 mutation slightly increased the responses at low ACh concentrations but gave half of the maximum response of wild-type AChRs. Hill coefficients and EC_{50}s (ACh concentrations that give 50% response of maximum normalized activity) for each dose-response curve, calculated as described in the Materials and Methods, are listed in Table 1. The Hill coefficients from the mutants shown in Table 1 are not significantly different from the wild-type value of 1.9, indicating that these mutants induce no dramatic changes in cooperativity.

The αTrp418 mutation increases desensitization rates

The αTrp418 mutant was further characterized as a prototype for the mutations, since this mutant had the largest effect on

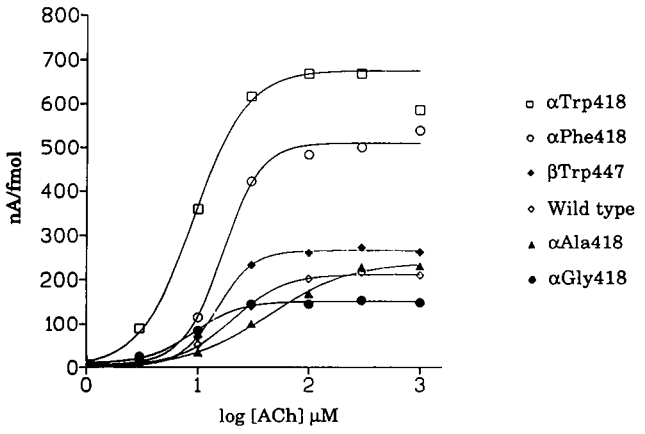

FIGURE 2 Representative dose-response relations for different *X. laevis* oocytes expressing wild-type or mutant AChRs. Currents are expressed as ACh-induced current (nA) per fmol of surface α-bungarotoxin binding sites. Data points were fitted to the Hill equation $Y = 100/[1 + (K_d/A)^n]$, where K_d is the apparent dissociation constant, equivalent to the EC_{50} or the ACh concentration inducing 50% maximal channel activity, n is the Hill coefficient, and A the ACh concentration.

receptor function. Representative sets of current responses in oocytes expressing wild-type or the αTrp418 mutant AChR are shown in Fig. 3 to illustrate the effects of the mutation on desensitization at different ACh concentrations. Desensitization rates increased with increasing ACh concentrations in oocytes expressing both wild-type and mutant AChRs. However, the αTrp418 mutant showed significantly faster desensitization rates compared with the wild type at all ACh concentrations. We used the average time for the current to decline to half of its peak amplitude, $t_{1/2}$, as an indication of the desensitization time course. Average $t_{1/2}$ values were more than fourfold longer in oocytes expressing wild-type AChR at 300 μM ACh ($t_{1/2} > 60 \pm 8$ s, $n = 3$) than in those expressing the αTrp418 mutant AChR ($t_{1/2} = 15 \pm 3$ s, $n = 5$).

The αTrp418 mutation increases channel open time

Patch clamp recordings of single-channel currents for the αTrp418 mutant showed a marked increase in mean open time compared with the wild-type (αCys418) channels. Fig. 4 *A* shows currents recorded from on-cell patches in oocytes expressing wild-type and the αTrp418 mutant AChRs. The increase in the duration of channel openings can be seen in the open time distributions for both channel types shown in Fig. 4, *C* and *D*. Note that the time scale for the mutant distribution has been compressed relative to the wild-type distribution. At 13 ± 1°C, our normal temperature for single-channel recording, wild-type channels showed a mean open time $\tau = 0.6 \pm 0.01$ ms ($n = 8$ patches; 4 batches of oocytes). The mean open time of the αTrp418 channels was $\tau = 16.5 \pm 0.06$ ms ($n = 10$ patches; 3 batches of oocytes), representing a 28-fold increase from wild type. At higher temperatures the apparent magnitudes of the increase in channel open time were somewhat less (e.g., ~23-fold at 17°C) but remained substantial at all temperatures between 11°C and 22°C. There was no significant difference for either wild-type or the αTrp418 receptor in channel conductance and open times recorded on different days after mRNA injection. Fig. 4 *B* shows that this mutation did not alter the permeability properties of the channel, since both the conductance and the reversal potentials were unchanged. The conductance value for the wild-type receptor was 65 ± 4 pS ($n = 9$ patches; 4 batches of oocytes) and for αTrp418 was 66 ± 2 pS ($n = 7$ patches; 3 batches of oocytes).

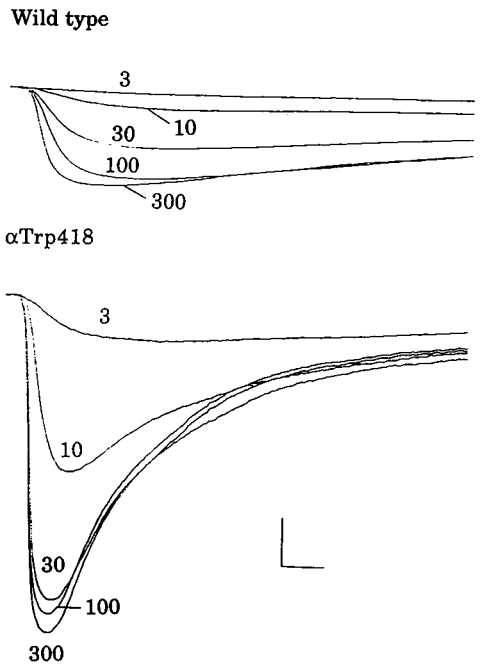

FIGURE 3 Representative current traces showing normalized ACh-induced current from wild-type and the αTrp418 receptors. ACh concentrations were 3, 10, 30, 100, and 300 μM as indicated on the figure. Currents are normalized to ACh-induced current per fmol of surface α-bungarotoxin binding sites. Calibration bars are 100 nA/fmol and 5 s. Desensitization rates of the mutant receptors are faster at all ACh concentrations.

DISCUSSION

The M4 domain of AChR is postulated to be at the lipid-protein interface but not part of the ion channel or ligand-binding domains (Pradier and McNamee, 1992). The ability of a single mutation at the postulated lipid-protein interface of the ACh receptor to dramatically alter ion channel function is a somewhat unexpected observation. Previous studies of lipid effects on AChR structure and function have suggested a significant linkage between lipid composition and receptor function (Fong and McNamee, 1987; Pradier and McNamee, 1992; Bhushan and McNamee, 1993), but specific effects at the amino acid level have not yet been proposed. We will focus the discussion on the αCys418 to αTrp418 mutant, because it had the largest effects on channel activity. Compared with wild-type receptor, the αTrp418 mutant increased the maximal normalized channel activity threefold, shifted the EC_{50} of the ACh dose-response curve from 32 μM to 13 μM, and increased desensitization rates. At the single-channel level, there was a 20- to 28-fold increase in channel mean open time. There were no changes in single-channel conductance, current-voltage relationships, or reversal potentials. Because of the dramatic change in channel open time, we examined a relatively simple kinetic model of AChR function to see whether the change in open time was sufficient to explain all the functional changes observed at both the single-channel and whole-cell level. The starting point for our analysis is

$$R \overset{K_1}{\rightleftharpoons} AR \overset{K_2}{\rightleftharpoons} A_2R \underset{\alpha}{\overset{\beta}{\rightleftharpoons}} A_2R^*$$

where R is the receptor, A is ACh, AR and A_2R are the mono- and bi-liganded species, and A_2R^* is the open (conducting) state of the receptor-ligand complex. K_1 and K_2 are the dissociation constants for the first and second ligand binding steps, respectively; β is the channel opening rate constant, and α is the channel closing rate constant (equal to 1/mean

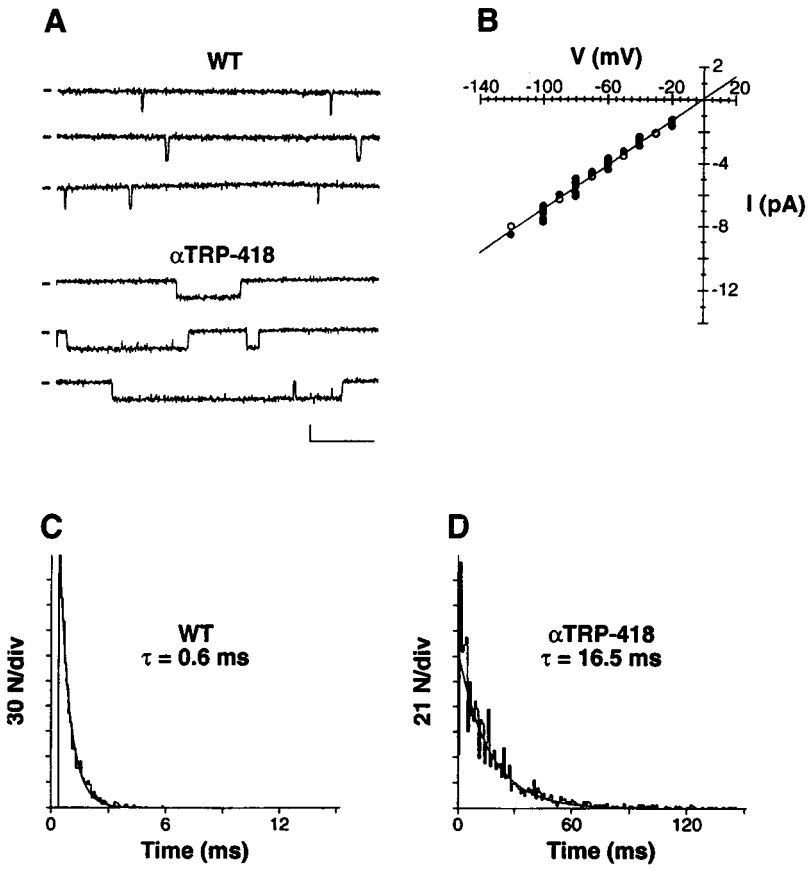

FIGURE 4 Mutation to αTrp418 increased channel open times but did not alter channel conductance. (*A*) Current records of channel openings from wild-type and the αTrp418 mutant AChRs recorded from on-cell patches. Holding potential was −80 mV, ACh concentration in the pipette was 4 μM, and the bath temperature was 12 ± 1°C for both records. Records were sampled at 100 μs and filtered at 4 kHz. Closed channel level is denoted at the beginning of each record by a small dash. Calibration bars are 5 pA and 20 ms. (*B*) Current-voltage relationship for wild-type (●) and the αTrp418 (○) AChRs. The mean conductance values were calculated from the slope of individual I-Vs and pooled together. wild-type conductance was $\gamma = 65 \pm 4$ pS ($n = 9$ patches; 4 oocyte batches) and the αTrp418 conductance was 66 ± 2 pS ($n = 7$ patches; 3 oocyte batches). The solid line represents the best fit line for the wild-type data. (*C*) A characteristic open time distribution for wild-type channels. This patch was held at −80 mV and kept at 14°C. The bin width in is 0.1 ms/div, and this distribution contains 1865 counts. The mean open time for this particular patch was 0.6 ± 0.01 ms. (*D*) Open time distribution for the αTrp418 channels. The patch was held at −80 mV and kept at 13°C. The mean open time for this patch is 16.5 ± 0.06 ms. The bin width was 1 ms/div; the histogram contains 2374 counts.

open time). According to the above scheme, the following equation is obtained:

$$\frac{[A_2R^*]}{R_{total}} = \frac{[A_2R^*]}{[R] + 2[AR] + [A_2R] + [A_2R^*]} \quad (1)$$

Letting $K_2 = aK_1$, where a is a constant, and simplifying, we have

$$\frac{[A_2R^*]}{R_{total}} = \frac{[A]^2}{(\alpha/\beta)(aK_1^2 + 2aK_1[A] + [A]^2) + [A]^2} \quad (2)$$

With given K_1, a, and α/β ratio, the theoretical dose-response curve for the AChR can be plotted. At high ACh concentrations, the maximum response is directly correlated with the α/β ratio. Letting the α/β ratio be 20-fold smaller than wild type (corresponding to a 20-fold decrease in the value of α) for the αTrp418 mutant can simulate the increase in maximal response and the decrease in EC_{50}. For example, changing the α/β ratio from a postulated value of 2 for wild type to 0.1 for the αTrp418 mutant could quantitatively explain the threefold increase in maximal response observed and also the decrease in EC_{50}. If the model is expanded to include channel blocking by ACh (Sine et al., 1990), lower values of the wild-type α/β ratio (e.g., 0.7 from their measurements in Ca^{2+}-free solution at 22°C) will also simulate an increase in maximal response and a decrease in EC_{50} when the α is reduced by a factor of 20. Thus a change in a single parameter (α) could account for all the observed macroscopic changes.

The increased rate of desensitization observed for the αTrp418 mutant could also be a consequence of the increased open time. Desensitization processes have been proposed from some (or all) of the closed states, from the open state, or from all states (Pradier and McNamee, 1992). If the rate of desensitization is proportional to the relative proportion of receptors in the A_2R^* state, this model predicts desensitization will be about threefold faster for the αTrp418 mutations than the wild-type AChR, in agreement with the fourfold difference in $t_{1/2}$ we measured. Thus, the data provide support for models in which the open channel form is a predominant pathway for desensitization as proposed by Cachelin and Colquhoun (1989).

Although the M4 segment of AChR is suggested to be located at the lipid-protein interface, it is not clear how mutations in this region alter ion channel function. A reasonable hypothesis is that mutations will alter helix-helix interactions. If the M4 is an α-helix as in Fig. 1, the amino residues on the right-hand side, which include the αCys418 in *Torpedo*, are more conserved among species and might interact with other domains. However, Blanton and Cohen (1992) showed that the amino residues on this side of the helix can be preferentially labeled by a nonspecific lipophilic probe, and they suggested that this side is exposed to lipid. It is remarkable that a mutation in a lipid-exposed region of an α-helix could have such dramatic effects on channel function. Recently, Unwin (1993b) reported that the M1, M3, and M4 regions of AChR might form β-sheet structures rather

than α-helix conformations based on observations from electron microscopy. Fourier transform infrared measurement from our laboratory (Butler and McNamee, 1993) also suggest a high content of β-sheet structure in the AChR. Our future studies will examine other positions in the M4 domain to identify patterns in modulating AChR function, with the goal of discerning the secondary structure of the M4 and allosteric linkages between the lipid-protein interface and the ion channel domain.

We thank Dr. Richard Nuccitelli for use of the facilities for oocyte injection and electrophysiological recordings and Barbara Birks for RNA preparation and oocyte injection.

This work was supported by National Institutes of Health Grant NS22941 to M.M.

REFERENCES

Barish, M. E. 1983. A transient calcium-dependent chloride current in the immature *Xenopus* oocyte. *J. Physiol. (Lond.).* 342:309–325.

Bertrand, D., A. Devillers-Thiery, F. Revah, J.-L. Galzi, N. Hussy, C. Mulle, S. Bertrand, M. Ballivet, and J.-P. Changeux. 1992. Unconventional pharmacology of a neuronal nicotinic receptor mutated in the channel domain. *Proc. Natl. Acad. Sci. USA.* 89:1261–1265.

Bhushan, A., and M. G. McNamee. 1993. Correlation of phospholipid structure with functional effects on the nicotinic acetylcholine receptor. *Biophys. J.* 64:716–723.

Blanton, M. P., and J. B. Cohen. 1992. Mapping the lipid-exposed regions in the *Torpedo californica* nicotinic acetylcholine receptor. *Biochemistry.* 31:3738–3750.

Butler, D. H., and M. G. McNamee. 1993. FTIR analysis of nicotinic acetylcholine receptor secondary structure in reconstituted membranes. *Biochem. Biophys. Acta.* 1150:17–24.

Cachelin, A. B., and D. Colquhoun. 1989. Desensitization of the acetylcholine receptor of frog end-plates measured in a vaseline-gap voltage clamp. *J. Physiol. (Lond.).* 415:159–188.

Charnet, P., C. Labarca, R. J. Leonard, N. J. Vogelaar, L. Czyzyk, A. Gouin, N. Davidson, and H. A. Lester. 1990. An open-channel blocker interacts with adjacent turns of α-helices in the nicotinic acetylcholine receptor. *Neuron.* 4:87–95.

Clarke, J. H., and M. Martinez-Carrion. 1986. Labeling of functionally sensitive sulfhydryl-containing domains of acetylcholine receptor from *Torpedo californica* membranes. *J. Biol. Chem.* 261:10063–10072.

Claudio, T., M. Ballivet, J. Patrick, and S. Heinemann. 1983. Nucleotide and deduced amino acid sequences of *Torpedo californica* acetylcholine receptor γ subunit. *Proc. Natl. Acad. Sci. USA.* 80:1111–1115.

Devillers-Thiery, A., J. Giraudat, M. Bentaboulet, and J.-P. Changeux. 1983. Complete mRNA coding sequence of the acetylcholine binding α-subunit of *Torpedo marmorata* acetylcholine receptor: a model for transmembrane organization of the polypeptide chain. *Proc. Natl. Acad. Sci. USA.* 80:2067–2071.

DiPaola, M., C. Czajkowski, and A. Karlin. 1989. The sidedness of the COOH terminus of the acetylcholine receptor delta subunit. *J. Biol. Chem.* 264:15457–15463.

Fong, T. M., and M. G. McNamee. 1987. Stabilization of acetylcholine receptor secondary structure by cholesterol and negatively charged phospholipids in membranes. *Biochemistry.* 26:3871–3880.

Galzi, J.-L., F. Revah, A. Bessis, and J.-P. Changeux. 1991. Functional architecture of the nicotinic acetylcholine receptor: from electric organ to brain. *Annu. Rev. Pharmacol.* 31:37–72.

Giraudat, J., C. Montecucco, R. Bisson, and J.-P. Changeux. 1985. Transmembrane topology of acetylcholine receptor subunits probed with photoreactive phospholipids. *Biochemistry.* 24:3121–3127.

Hamill, O. P., A. Marty, E. Neher, B. Sakmann, and F. J. Sigworth. 1981. Improved patch clamp techniques for high resolution current recording from cells and cell-free membrane patches. *Pfluegers Arch.* 391: 85–100.

Heasman, J., S. Holwill, and C. C. Wylie. 1991. Fertilization of cultured *Xenopus* oocyte and use in studies of maternally inherited molecules. *In* Methods in Cell Biology. Vol. 36: *Xenopus laevis*: Practical Uses in Cell and Molecular Biology. B. K. Kay and H. B. Peng, editors. Academic Press, San Diego. 213–230.

Horton, R. M., and L. R. Pease. 1991. Recombination and mutagenesis of DNA sequence using PCR. *In* Directed Mutagenesis. M. J. McPherson, editor. IRL Press, New York. 217–246.

Hucho, F., W. Oberthur, and F. Lottspeich. 1986. The ion channel of the nicotinic acetylcholine receptor is formed by the homologous helices MII of the receptor subunits. *FEBS Lett.* 205:137–142.

Huganir, R. L., and E. Racker. 1982. Properties of proteoliposomes reconstituted with acetylcholine receptor from *Torpedo californica*. *J. Biol. Chem.* 257:9372–9378.

Imoto, K., C. Busch, B. Sakmann, M. Mishina, T. Konno, J. M. Nakai, H. Bujo, Y. Mori, M. Fukuda, and S. Numa. 1988. Rings of negatively charged amino acids determine the acetylcholine receptor channel conductance. *Nature.* 335:645–648.

Kao, P. N., A. J. Dwork, R. J. Kaldany, M. L. Silver, J. Wideman, S. Stein, and A. Karlin. 1984. Identification of the a subunit half-cystine specifically labeled by an affinity reagent for the acetylcholine receptor binding site. *J. Biol. Chem.* 259:11662–11665.

Kao, P. N., and A. Karlin. 1986. Acetylcholine receptor binding site contains a disulfide crosslink between adjacent half-cystinyl residues. *J. Biol. Chem.* 261:8085–8088.

Leonard, R. J., C. G. Labarca, P. Charnet, N. Davidson, and H. A. Lester. 1988. Evidence that the M2 membrane-spanning region lines the ion channel pore of the nicotinic receptor. *Science (Washington DC).* 242: 1578–1581.

Li, L., Y.-H. Lee, P. Pappone, A. Palma, and M. G. McNamee. 1992. Site-specific mutations of nicotinic acetylcholine receptor at the lipid-protein interface dramatically alter ion channel gating. *Biophys. J.* 62: 61–63.

Li, L., M. Schuchard, A. Palma, L. Pradier, and M. G. McNamee. 1990. Functional role of the cysteine 451 thiol group in the M4 helix of the γ subunit of *Torpedo californica* acetylcholine receptor. *Biochemistry.* 29: 5428–5436.

Lingle, C. J., D. Maconochie, and J. H. Steinbach. 1992. Activation of skeletal muscle nicotinic acetylcholine receptors. *J. Membr. Biol.* 123: 195–217.

Lo, D. C., J. L. Pinkham, and C. F. Stevens. 1991. Role of a key cysteine residue in the gating of the acetylcholine receptor. *Neuron.* 6:31–40.

Marquez, J., A. Iriarte, and M. Martinez-Carrion. 1989. Covalent modification of a critical sulfhydryl group in the acetylcholine receptor: cysteine-222 of the α-subunit. *Biochemistry.* 28:7433–7439.

Mishina, M., T. Tobimatsu, K. Imoto, et al. 1985. Location of functional regions of acetylcholine receptor α-subunit by site-directed mutagenesis. *Nature.* 313:364–369.

Mosckovitz, R., and J. M. Gershoni. 1988. Three possible disulfides in the acetylcholine receptor α-subunit. *J. Biol. Chem.* 263:1017–1022.

Noda, M., H. Takahashi, T. Tanabe, M. Toyosato S. Kikyotani, Y. Furutani, T. Hirose, H. Takashima, S. Inayama, T. Myata, and S. Numa. 1983. Structural homology of *Torpedo californica* acetylcholine receptor subunits. *Nature.* 302:528–532.

Pedersen, S. E., S. D. Sharp, W.-S. Liu, and J. B. Cohen. 1992. Structure of the noncompetitive antagonist-binding site of the *Torpedo* nicotinic acetylcholine receptor: [3H]meproadifen mustard reacts selectively with α-subunit Glu-262. *J. Biol. Chem.* 267:10489–10499.

Pradier, L., and M. G. McNamee. 1992. The nicotinic acetylcholine receptor. *In* The Structure of Biological Membranes. P. Yeagle, editor. Telford, Caldwell, NJ. 1047–1106.

Pradier, L., A. S. Yee, and M. G. McNamee. 1989. Use of chemical modifications and site-directed mutagenesis to probe the functional role of thiol groups on the γ subunit of *Torpedo californica* acetylcholine receptor. *Biochemistry.* 28:6562–6571.

Revah, F., D. Bertrand, J.-L. Galzi, A. Devillers-Thiery, C. Mulle, N. Hussy, S. Bertrand, M. Ballivet, and J.-P. Changeux. 1991. Mutations in the channel domain alter desensitization of a neuronal nicotinic receptor. *Nature.* 353:846–849.

Revah, F., J.-L. Galzi, J. Giraudat, P.-Y. Haumont, F. Lederer, and J.-P. Changeux. 1990. The non-competitive blocker [^{3}H]chlorpromazine labels three amino acids of the acetylcholine receptor γ subunit: implications for the α-helical organization of regions MII and for the structure of the ion channel. *Proc. Natl. Acad. Sci. USA.* 87:4675–4679.

Sine, S. M., T. Claudio, F. J. Sigworth. 1990. Activation of *Torpedo* acetylcholine receptor expressed in mouse fibroblasts. *J. Gen. Physiol.* 96: 395–437.

Stroud, R. M., M. P. McCarthy, and M. Shuster. 1990. Nicotinic acetylcholine receptor superfamily of ligand-gated ion channels. *Biochemistry.* 29:11009–11023.

Unwin, N. 1993a. Neurotransmitter action: opening of ligand-gated ion channels. *Neuron.* 10(Suppl.):31–41.

Unwin, N. 1993b. Nicotinic acetylcholine receptor at 9 Å resolution. *J. Mol. Biol.* 229:1101–1124.

Villarroel, A., S. Herlitze, M. Loenen, and B. Sakmann. 1991. Location of a thionine residue in the α-subunit M2 transmembrane segment that determines the ion flow through the acetylcholine receptor channel. *Proc. R. Soc. Lond. B Biol. Sci.* 243:69–74.

Villarroel, A., and B. Sakmann, 1992. Threonine in the selectivity filter of the acetylcholine receptor channel. *Biophys. J.* 62:209–221.

Wallace, R. A., D. W. Jared, J. N. Dumont, and M. W. Sega. 1973. Protein incorporation by isolated amphibian oocytes. III. Optimum incubation conditions. *J. Exp. Zool.* 184:321–334.

White, M. M., and M. Aylwin. 1987. Niflumic and flufenamic acids are potent reversible blockers of Ca^{2+}-activated Cl^- channels in *Xenopus oocytes. Mol. Pharmacol.* 37:720–724.

Yee, A. S., D. E. Corley, and M. G. McNamee. 1986. Thiol-group modification of *Torpedo californica* acetylcholine receptor: subunit localization and effects on function. *Biochemistry.* 25:2110–2119.